Original Article

Flow of a Casson Fluid with Heat Transfer over a Shrinking Sheet and its Dual Solutions

Debasish Dey [I] and Rupjyoti Borah[II*]

[I] Department of Mathematics, Assistant Professor, Dibrugarh University, Dibrugarh-786004, Assam, India

[II] Department of Mathematics, Research Scholar, Dibrugarh University, Dibrugarh-786004, Assam, India

Emails: [I] debasish41092@gmail.com and [II*] rpjtbrh@gmail.com

Abstract

An effort has been addressed to examine the dual solutions of boundary layer flow of the Casson fluid over a shrinking sheet with the effects of Joule heating and power-law heat flux. A homogeneous magnetic field is implemented in the system along the normal direction of the flow. An appropriate similarity transformations are employed to renovate the supported equations of the present problem into a set of solvable form and hence solved these equations using the three-stage Lobatto IIIa method by developing a numerical bvp4c code in MATLAB. Due to the shrinking surface, some disturbances occur on the flow which gives two different solutions; one is stable and another one is unstable. Graphical results have been shown to analyze velocity and temperature fields. The stability analysis is executed to characterize the stable and physically attainable solution. It is perceived that the Casson fluid parameter helps to enhance the speed and temperature of the fluid during the time-independent case. But, it controls the motion as well as the temperature of the fluid during the time-dependent case.

Keywords: Magnetohydrodynamics, Casson fluid, Dual solutions, Heat transfer, Joule heating, Stability analysis

1. Introduction

In the recent times, there are multifarious appliance of non-Newtonian fluid in different areas such as engineering sciences and industrial processes. Again, a huge number of research on boundary layer flow of non-Newtonian fluids with the effects of both thermal and mass diffusivity are available in the recent time. Mechanics of non-Newtonian fluid flows preserve a special confront to engineers, physicists and mathematician due to complexity and vast significance of these fluid in physical fields. The Casson fluid is a sub class of non-Newtonian fluid which has spacious significance in food processing, metallurgy, drilling operations and bio-engineering etc. Some important paradigms of this fluid are honey, concentrated fruit juice, blood and tomato sauce etc. This type of fluid has yield stress and the characteristics of this fluid is completely dependent on shear stress and yield stress. If the applying shear stress to the fluid is smaller than the yield stress, then this type of fluid has infinite viscosity for that it behaves like a solid. Again, it behaves like a liquid when the shear stress is larger than the applying yield stress to the fluid. Amilmohamadi, Akram, and Sadeghy (2016), Zaib, Bhattacharyya, Uddin, and Shafie (2016), Tamoor, Waqas, Khan, Alsaedi, and Hayat (2017), Maraj, Faizan, and Shaiq (2019) and Shah, Kumam, and Deebani (2020) have put their ideas and given physical significance of the Casson fluid flow in different physical areas by taking different geometries. Oke, Mutuku, Kimathi, and Animasaun (2020) have investigated the Casson fluid under the action of Cariolis force and its importance in different fields by considering rotating non-uniform surface. Alghamdi *et al.* (2020) have investigated the boundary-layer flow of Casson hybrid nanofluid streaming above an elongating surface. They have concluded that this fluid model with the hybrid nanoparticles is very important for the enhancement of thermal conductivity that is a key requirement for the modern industries. Nandeppanavar, M.C., and Raveendra (2021) have examined the simultaneous influence of both thermal and mass transfers of the Casson fluid flow with variable thermal radiation.

The flow due to the shrinking surface along with the effects of both thermal and mass diffusivity have taken a great deal of interest in engineering sciences, industrial processes and many other areas. Some examples are wire drawing, extrusion, metal spinning and hot rolling etc. Application of both heat and mass transfer over stretching/shrinking surface is annealing and thickening of copper wire. The boundary-layer flow over contracting/moving surface was first introduced by Crane (1970). The researchers, Krishna, Reddy, and Makinde (2018), Sarkar *et al.* (2019), Anuradha and Punithavalli (2019), Vaidya *et al*. (2020), Dey and Chutia (2021), Dey and Hazarika (2021) and Dey, Borah, and Mahanta (2021) have discussed the boundary layer flow of different fluid models due to stretching/shrinking type surfaces and their importance in different areas. They have also investigated the thermal transference of the fluid flow with their importance in different fields. In the recent times, the Joule heating and heat source effect and magnetohydrodynamics on this present model are found in different importance applications in different physical areas. Many researchers, Hayat, Shafiq, and Alsaedi (2014), Khan, Khan, Irfan, and Alshomrani (2017), Saidulu and Lakshmi (2017) and Ibrahim, Kumar, Lorenzini, and Lorenzini (2019) have analysed the consequence of Joule heating and heat source effects by taking different surfaces. Adnan, Arifin, Bachok, and Ali (2019) have discussed the importance of the shrinking type surface during the fluid streaming above the geometries. The effects of the magnetic field during the fluid flow of this model have many industrial applications such as MHD (magneto-hydrodynamics) pump and MHD generators etc. Zehra *et al*. (2021) have investigated the Casson nanofluid flow over a curved stretching/shrinking channel with homogeneous magnetic field. Jamshed *et al*. (2021) have explored the ideas of the magnetized fluid streaming above an shrinking/stretching surfaces by employing the Casson fluid model.

Markin (1980) have introduced the dual type solutions and found that upper branch i.e., the time dependent solution is unstable. After that, a huge amount of literatures on boundary layer flow and their dual solutions have been achieved in the research areas. Many researchers, Najib, Bachok, and Arifin (2017), Ahmed, Siddique, and Sagheer (2018), Salleh, Bachok, Arifin, Ali, and Pop (2018), Dey and Borah (2020) and Mishra, Hussain, Seth, and Makinde (2020) have analysed the dual solutions and their stability. They have found two types of solutions and interpreted that the time independent solution is stable in nature and physically achievable. Dey and Borah (2021) have investigated the numerical solutions of the two-fold solutions of the fluid flow caused due to an elongating surface under the action of both thermal and mass transmission by considering the second-grade fluid. Dey, Makinde, and Borah (2022) have scrutinized the nature of the dual solutions and their occurrence during the flow of the fluid under the effects of both thermal and mass transference by placing stretching/shrinking surface. Dey, Borah, and Khound (2022) have studied the dual solutions and their stability analysis of the Casson fluid flow over an elongating sheet. They have found that the first solution which is responsible for time-independent case is stable and physically tractable. All the aforesaid literature have studied about the impacts of magnetic field in the different fluid flow caused due to stretching/shrinking surfaces.

In fluid mechanics, all the flow problems have been elaborated by some physical principles of conservations. This physical laws give leading mathematical equations that describe the pattern of the motion, temperature as well as mass transmission of the fluid. These supported equations are highly non-linear, so it can't be too easy to solve this problem by analytical approach. In this study, we have adopted the three-stage Lobatto IIIa formula [referring Shampine, Kierzenka, and Reichelt (2000)] for solving the boundary value problems by developing a numerical bvp4c codes in MATLAB. Many researchers such as Dey and Borah (2020, 2021) and Dey, Hazarika, Borah (2021) have applied the MATLAB routine bvp4c solver scheme to come out from their studies.

The objective of this problem is to explore the nature of dual solutions of the Casson fluid flow due to contracting sheet with the causes of joule heating and heat source. A constant magnetic field is applied in the normal direction of the flow. Adopting suitable similarity transformations, a third order differential equation corresponding to flow equation and a second order equation corresponding to heat transfer equation are developed. The numerical calculations and visualization are carried out for different flow parameters by using MATLAB built-in bvp4c solver scheme. Numerical results have been confirmed with the previous results of Jaber (2016) for a certain case and the comparison is found to be in excellent agreement. The nature of dual solutions and their stability, the Casson fluid flow due to contracting surface are the novelty of this work.

2. Formulation of the Problem

The following assumptions are taken to formulate this present problem in terms of mathematical equations. The flow diagram of this problem is shown in figure (1).

(i) 2D, time-independent and incompressible flow of Casson fluid over a shrinking sheet,

(ii) A constant magnetic field of strength (B_0) is applied in the vertical direction of the sheet,

(iii) The flow is induced by the (a) inertia force, (b) viscous force, (c) pressure gradient and (d) Lorentz force,

(iv) The contracting sheet is characterized by the velocity of the fluid $u = -cx$, where the constant $c > 0$ represents the shrinkage of the sheet at $y = 0$ and

(v) In heat transfer, the flow is maintained by both free convection and conduction, heat generation, dissipation of energy and joule heating with prescribed wall temperature $T_w(x) = T_\infty + Bx^2\sqrt{\upsilon c^{-1}}$.

(vi) The constitutive equation of the present fluid model [referring Lund, Omar, Khan, Baleanu, and Nisar (2020)] which represents the isotropic and incompressible progression of the fluid is stated as:

$$\tau_{ij} = \begin{cases} 2\left(\mu_B + \dfrac{P_y}{\sqrt{2\pi}}\right)e_{ij}, & \pi > \pi_c \\ 2\left(\mu_B + \dfrac{P_y}{\sqrt{2\pi_c}}\right)e_{ij}, & \pi < \pi_c \end{cases}$$

where, the plastic dynamic viscosity of this fluid model is meant by μ_B, $\pi = e_{ij}e_{ij}$ is the $(i, j)^{th}$ deformation rate of the fluid, π_c the critical value of the deformation rate and the yield stress of the fluid is meant by P_y.

(vii) One of the most important force which induce the present fluid model streaming above a contracting surface is Lorentz force that can be expressed as

$$\vec{F} = q\,\vec{v} \times \vec{B}.$$

where, $\vec{B} = B_0 y$ is the magnetic field that can be applied in the normal direction of the flow and q the charge and $\vec{v}$ the velocity vector.

Following boundary layer theory, the foremost equations of this study are:

$$\frac{\partial u}{\partial x} + \frac{\partial v}{\partial y} = 0, \tag{1}$$

$$u\frac{\partial u}{\partial x} + v\frac{\partial u}{\partial y} = \upsilon\left(1+\frac{1}{\beta}\right)\frac{\partial^2 u}{\partial y^2} - \frac{\sigma B_0{}^2}{\rho}u, \tag{2}$$

$$u\frac{\partial T}{\partial x} + v\frac{\partial T}{\partial y} = \frac{k}{\rho C_P}\frac{\partial^2 T}{\partial y^2} + \frac{Q*}{\rho C_P}\left(T - T_\infty\right) - \frac{\mu_\beta}{\rho C_P}\left(1+\frac{1}{\beta}\right)\left(\frac{\partial u}{\partial y}\right)^2 + \frac{\sigma B_0{}^2}{\rho C_P}u^2. \tag{3}$$

The conditions at the surface are:

$$\begin{gathered} y = 0 : u = cx, v = -v_0, \frac{\partial T}{\partial y} = Bx^2; \\ y \to \infty : u \to 0, v \to 0, T \to T_\infty. \end{gathered} \tag{4}$$

Where, c is the constant and its negative value recognizes shrinkage of the sheet at the surface.

The following similarity transformations are employed to remodel the equations [(1)-(3)].

$$u = cxf'(\eta), v = -\sqrt{\upsilon c}\, f(\eta), \eta = \sqrt{c\upsilon^{-1}}\, y, \theta(\eta) = \frac{T - T_\infty}{T_W - T_\infty}. \tag{5}$$

The equation (1) is clearly hold and other two equations become in the following form:

$$\left(1+\frac{1}{\beta}\right)f''' + ff'' - f'^2 - Mf' = 0, \tag{6}$$

$$\theta'' + \Pr f\theta' - 2\Pr f'\theta - \Pr H\theta + \Pr Ec\left(1+\frac{1}{\beta}\right)f''^2 + EcJf'^2 = 0. \tag{7}$$

The boundary condition (4) becomes:

$$\begin{aligned} &\eta = 0: f(\eta) = s, f'(\eta) = -1, \theta'(\eta) = 1; \\ &\eta \to \infty: f'(\eta) \to 0; \theta(\eta) \to 0. \end{aligned} \tag{8}$$

The flow parameters that are involved in this investigation are defined in the following way:

$$s = \frac{v_0}{\sqrt{c\eta}}, \Pr = \frac{\mu C_P}{k}, M = \frac{\sigma B_0^{\,2}}{\rho c}, Ec = \frac{c\sqrt{c}}{BC_P\sqrt{\upsilon}}, J = \frac{\sigma B_0^{\,2}\mu C_P}{\rho^2 k}, H = \frac{\upsilon Q^*}{C_P c\rho} \,\&\, \beta = \frac{\mu_B\sqrt{2\pi_c}}{P_y}.$$

The following physical quantities are observed in this study that are very important in several physical areas such as engineering sciences and industrial processes. The skin friction coefficient (C_f) and the Nusselt number (rate of heat transfer) (Nu) are defined in the following way:

$$C_f = \frac{\mu\left(1+\frac{1}{\beta}\right)}{\rho u_w^{\,2}}\left(\frac{\partial u}{\partial y}\right)_{y=0} \,\&\, Nu = -\frac{x}{(T_w - T_\infty)}\left(\frac{\partial T}{\partial y}\right)_{y=0}. \tag{9}$$

Then we have,

$$C_f = \frac{\mu\left(1+\frac{1}{\beta}\right)x}{\rho\sqrt{\upsilon c}} f''(0) \,\&\, Nu = -Bx^3\theta'(0). \tag{10}$$

3. Flow Stability

To characterize the more stable and physically attainable solution, the time dependent governing equations are needed. So, we have considered the unsteady form of governing equations (2) and (3) by adding the terms $\frac{\partial u}{\partial t} \,\&\, \frac{\partial T}{\partial t}$ in (2) and (3) respectively. To solve the unsteady form of governing equations, the following new similarity transformations are employed:

$$u = cxf'(\eta,\tau), v = -\sqrt{\upsilon c}\, f(\eta,\tau), \eta = \sqrt{c\upsilon^{-1}}\, y, \theta(\eta,\tau) = \frac{T - T_\infty}{T_W - T_\infty} \,\&\, \tau = ct. \tag{11}$$

Where, t is the time. After applying the equation (11) into the unsteady governing equations, we have achieved the following set of equations:

$$\left(1+\frac{1}{\beta}\right)\frac{\partial^3 f}{\partial \eta^3}+f(\eta,\tau)\frac{\partial^2 f}{\partial \eta^2}-\left(\frac{\partial f}{\partial \eta}\right)^2-M\frac{\partial f}{\partial \eta}-\frac{\partial^2 f}{\partial \eta \partial \tau}=0, \tag{12}$$

$$\frac{\partial^2\theta}{\partial \eta^2}+\Pr f(\eta,\tau)\frac{\partial \theta}{\partial \eta}-2\Pr\frac{\partial f}{\partial \eta}\theta(\eta,\tau)-H\theta(\eta,\tau)+\Pr Ec\left(1+\frac{1}{\beta}\right)\left(\frac{\partial^2 f}{\partial \eta^2}\right)^2+EcJ\left(\frac{\partial f}{\partial \eta}\right)^2-\Pr\frac{\partial \theta}{\partial \tau}=0, \tag{13}$$

the pertinent boundary conditions are:

$$\begin{aligned}&\frac{\partial f}{\partial \eta}(0,\tau)=-1,\ f(0,\tau)=s,\frac{\partial \theta}{\partial \eta}(0,\tau)=1;\\&\frac{\partial f}{\partial \eta}(\infty,\tau)\to 0,\theta(\infty,\tau)\to 0.\end{aligned} \tag{14}$$

Following Markin (1980) and Weidman and Awaludin (2016), the following perturb (separation of variables) equations are considered which helps to simplify the equations (12) and (13) and transform into a set of linearized form.

$$\begin{aligned}&f(\eta,\tau)=f_0(\eta)+e^{-\lambda\tau}F(\eta,\tau),\theta(\eta,\tau)=\theta_0(\eta)+e^{-\lambda\tau}G(\eta,\tau),\\&\phi(\eta,\tau)=\phi_0(\eta)+e^{-\lambda\tau}H(\eta,\tau).\end{aligned} \tag{15}$$

where, $f_0\ \&\ \theta_0$ are the solutions of the time free equations and $F\ \&\ G$ the small relative to steady flow solutions and λ the unknown eigen-value parameter. To obtain the steady flow solutions, we have to set $\tau\to 0$, which give $F=F_0\ \&\ G=G_0$. Therefore, we have perceived the following set of linearized eigen-value problems.

$$\left(1+\frac{1}{\beta}\right)F_0'''+\left(f_0F_0''+F_0f_0''\right)-2f_0'F_0'-MF_0'+\lambda F_0'=0, \tag{16}$$

$$\begin{aligned}&G_0''+\Pr\left(f_0G_0'+F_0\theta_0'\right)-2\Pr\left(f_0'G_0+F_0'\theta_0\right)-HG_0+2\Pr Ec\left(1+\frac{1}{\beta}\right)f_0''F_0''+2EcJ\Pr f_0'F_0'\\&+\Pr\lambda G_0=0,\end{aligned} \tag{17}$$

and the conditions at the surface become

$$F_0'(0)=0,F_0(0)=0,G_0'(0)=0;F_0'(\infty)\to 0,G_0(\infty)\to 0. \tag{19}$$

Solving these equations, we have got infinite set of eigen values. Among these eigen values, the positive smallest eigen value represents initial decay of disturbances on the flow and hence the flow will be in stable nature. If the least eigen value is found to be negative, then an initial growth of disturbances is happened on the flow and hence the flow will be in unstable in nature. To evaluate the fixed eigen values, we have relaxed the boundary condition $F_0\,'(\infty) \to 0$ into a new boundary condition $F_0\,''(0) = 1$ [following Harish, Ingham, and Pop (2009) and Weidman and Awaludin (2016)].

4. Discussion of the results

The "MATLAB built in bvp4c solver technique" is taken up to work out this problem [following Shampine, Kierzenka, and Reichelt (2000), Dey and Hazarika (2020) and Dey and Chutia (2020)]. The non-dimensional Prandtl number $(\Pr)$ is fixed to 0.72 throughout this investigation which physically signifies the higher thermal conductivity materials-air ($\Pr = 0.7 < 1$, thermal diffusivity is greater than momentum diffusivity) [referring Salleh, Bachok, Arifin, Ali, and Pop (2010)]. The visualization of flow behaviours are made in terms of graphs with different values of flow parameters. A special highlights are given on the Casson fluid parameter (β) such that its value $\beta \to \infty$ recognize the Newtonian fluid, heat source parameter (H) and Joule heating parameter (J).

Verification of the results:

To validate our results, we have compared our numerical values of the shear stress at the surface for the steady Newtonian fluid $(\beta \to \infty)$ in the case of stretching sheet with the pioneer work of Jaber (2016). Table (1) shows a very good conformity of our results. This conformity help us to work out the other results.

The numerical values of smallest eigen value is tabulated in table (2). From this table, it seen that least eigen values for the steady flow solution are positive. It decays the initial disturbances on the flow and consequently the steady flow solution is stable. But, for unsteady solution, the smallest eigen values are found to be negative which generates the disturbances on the flow and the flow is unstable.

Figures (2) and (3) are depicted to illustrate the motion and temperature of the fluid for developing values of the Casson fluid parameter (β). From figure (2), it is perceived that the enhancing values of β accelerates the motion of the fluid during both the time-independent and time-dependent cases. Generally, enhancement of β decelerates the motion of the fluid because it raises the plastic dynamic viscosity. But an opposite behaviour is observed during the flow and this happens only because of the considering geometry (shrinking surface). From figure (3), it is noticed that temperature of the fluid reduces during the flow with β. This can be physically ascribed that higher values of β enhances the resistance of the fluid and reduces the effects of yield stress on the fluid and hence temperature pattern get slower during both the cases. Further, it can be concluded that during time-dependent case, the velocity and temperature of the fluid converge to its free stream region more quickly than the time-independent case. Due to the appliance of magnetic meadow on the system, the speed of the motion during both the cases (steady and unsteady cases) accelerates [shown in figure (4)]. It can be physically attributed that enhancing values of magnetic parameter reduce the effects of viscosity of the fluid at the surface and dominate the Lorentz force and hence speed of the fluid increases. From figure (5), it is seen that both the solutions (steady and unsteady solutions) of the temperature distribution of the fluid enhance near the surface of the sheet with M. It can be physically justified that enlarging values of M enhance the magnetic force as well as friction of the fluid and hence the temperature pattern of the fluid during both the cases increases. Also, maximum variation of the temperature field of the fluid is seen in the region $0 < \eta < 0.5.$ Figure (6) is portrayed to investigate the nature of speed of the fluid due to the effects of suction parameter $(s > 0).$ Increasing values s enhances the speed of the fluid during both the cases. Again, it is observed that the speed of the fluid during steady case is completely negative for various values of $s.$ From this figure, it is also perceived that the speed of the fluid during time-dependent case gets oscillation in the region $2 < \eta < 10$ with the increasing values of $s.$ This happens only because of the additional fluid suctioned by the system and the considering geometry that shrinkage in the opposite direction of the flow.

The consequences of heat source and Joule heating parameters on temperature distribution are plotted in figures (7) and (8) respectively. From figure (7), it is perceived that the temperature of the fluid decreases with the improving values of H during both the time-independent and time-dependent solutions. Generally, developing values of H generates an additional heat in the system and hence the temperature pattern of the fluid enriches. But, an opposite nature is seen during this study because the considering geometry shrink in the opposite direction of the flow. Also, it is seen that maximum temperature of the fluid generates in the vicinity of the surface and then gradually going to its free stream region at which both the solution are same manner. The temperature of the fluid during both steady and unsteady cases accelerate with developing values of Joule heating parameter $(J).$ It is also noticed that the thermal boundary layer width during steady solution is more thinner as compared to the unsteady (time-dependent) solution. All the figures satisfy the far field boundary conditions asymptotically. Also, we have seen that both the solution exists up to some certain region of the similarity variables η. Again, the steady solution is occurred in the vicinity of the surface and converges to its free stream region than the unsteady solutions, so the steady solution is more realizable than the unsteady solution.

5. Conclusions

In this study, we have investigated the two-fold solutions of the thermally stratified Casson fluid streaming above a contracting surface under the influence of magnetic field. The pertinent flow parameters discussed in the result section of this study have multifarious applications in different physical areas. Again, the considering fluid model is one of the most important area for the recent research trends. The scientists and industrialists may use this fluid model under the influence of different flow factors such as magnetic field, Joule heating, heat source and suction/injection for achieving more benefits. The following major keys observed in this study are:

- All the profiles satisfy the far-field boundary conditions asymptotically and exists dual type solutions up to certain region of the similarity variables η.
- From the stability point of view, it is perceived that the steady flow solutions is stable and the unsteady flow solution is unstable.
- The Casson fluid parameter has major significance to develop the speed of the fluid as well as to control the temperature of the fluid for which we can save the system from damage.
- Influence of magnetic parameter enhances the motion of the fluid during both the cases (both time-independent and time-dependent cases). Again, increasing values of magnetic parameter develops the temperature field of the fluid.
- The Joule heating parameter enhances the entire temperature field of the system.

- We can control the temperature of the fluid by utilizing the heat source parameter.
- The suction of the fluid in the system develops the motion of the fluid during both steady and unsteady case.

“ Nomenclature:

c	constant
B	constant
$f'(\eta)$	dimensionless velocity
Ec	Eckert number
H	heat source parameter
$Q*$	heat generation parameter
J	Joule heating parameter
B_0	magnetic field (T)
M	Magnetic parameter
Nu	Nusselt number
$\Pr$	Prandtl number
u	rate of displacement along x-directions (m/s)
v	rate of displacement along y-directions (m/s)
C_P	specific heat at constant pressure
v_0	suction/injection parameter
s	suction/injection parameter
C_f	skin friction coefficient
T	temperature of the fluid (K)
t	time variable (s)
k	thermal conductivity (m^2/s)
P_y	yield stress of the fluid (MPa)

Greek Symbols:

β	Casson fluid parameter
ρ	density (kg/m^3)
τ	dimensionless time variable
$\theta(\eta)$	dimensionless temperature field
σ	electric density of the fluid (s/m)
υ	kinematic viscosity (m^2/s)
υ	kinematic viscosity (m^2/s)
μ_β	plastic dynamic viscosity (pa.s)
η	similarity variable
ψ	stream function
λ	unknown eigen-value parameter

Suffix:

w	at wall

∞ at free stream region”

Reference

Adnan, N.S.M., Arifin, N.M., Bachok, N. & Ali, F.M. (2019). Stability analysis of MHD flow and heat transfer passing a permeable exponentially shrinking Sheet with partial slip and thermal radiation. *CFD Letters*, 12, 34-42.

Ahmed, A., Siddique, J. I. & Sagheer, M. (2018). Dual solutions in a boundary layer flow of a power law fluid over a moving permeable flat plate with thermal radiation, viscous dissipation and heat generation/absorption. *Fluids*, 3(1).

Alghamdi, W., Gul, T., Nullah, M., Rehman, A., Nasir, S., Saeed, A. & Bonyah, E. (2020). Boundary layer stagnation point flow of the casson hybrid nanofluid over an unsteady stretching surface. *AIP Advances*, 11, 015016.

Amlimohamadi, H., Akram , M. & Sadeghy, K. (2016). Flow of a casson fluid through a locally-constricted porous channel: a numerical study. *Korea Australia Rheology Journal*, 28(2),129–137.

Anuradha, S. & Punithavalli, R. (2019). MHD boundary layer flow of a steady micro polar fluid along a stretching sheet with binary chemical reaction. *International Journal of Applied Engineering Research*, 14(2), 440–446.

Crane, L. J. (1970). Flow past a stretching plate. *Zeitschrift für Angewandte Mathematik und Physik ZAMP*, 21(4), 645–647.

Dey, D. & Borah, R. (2020). Dual solutions of boundary layer flow with heat and mass transfers over an exponentially shrinking cylinder: stability analysis. *Latin American Applied Research*, 50(4), 247–253.

Dey, D. & Hazarika, M. (2020). Entropy generation of hydro-magnetic stagnation point flow of micropolar fluid with energy transfer under the effect of uniform suction / injection. *Latin American Applied Research*, 50 (3), 209–214.

Dey, D. & Chutia, B. (2020). Dusty nanofluid flow with bioconvection past a vertical stretching surface. *Journal of King Saud University- Engineering Sci*ences. DOI:10.1016/j.jksues.2020.11.001

Dey, D. & Borah, R. (2021). Stability analysis on dual solutions of second-grade fluid flow with heat and mass transfers over a stretching sheet. *International Journal of Thermofluid Science and Technology*, 8(2), 080203.

Dey, D. & Chutia, B. (2021). Modelling of multi-phase fluid flow with volume fraction past a permeable stretching vertical cylinder and its numerical study. *Latin American Applied Research*, 51(3), 165-171.

Dey, D., Hazarika, M. & Borah, R. (2021). Entropy generation analysis of magnetized micropolar fluid streaming above an exponentially extending plane. *Latin American Applied Research*, 51(4), 255-260.

Dey, D. & Hazarika, M. (2021). Second law analysis of pseudo-plastic nanofluid stream past a stretching sheet with a sliding consequence. *Heat Transfer,* 1-15.

Dey, D., Makinde, O.D. & Borah, R. (2022). Analysis of dual solutions in MHD fluid flow with heat and mass transfer past an exponentially stretching/shrinking surface in a porous medium. *Int. J. Appl. Comput. Math*, 8(66), https://doi.org/10.1007/s40819-022-01268-7.

Dey, D., Borah, R. & Khound, A.S. (2022). Stability analysis on dual solutions of MHD Casson fluid flow with thermal and chemical reaction over a permeable elongating sheet. *Heat Transfer*,51(4), 3401-3417.

Hayat, T., Shafiq, A. & Alsaedi, A. (2014). Effect of joule heating and thermal radiation in flow of third grade fluid over radiative surface. *PLoS One*, 9(1), 1–12.

Harish, S.D., Ingham, D.B. & Pop. I, (2009). Mixed convection boundary layer flow near the stagnation point on a vertical surface in a porous medium: Brinkman model with slip. *Transport Porous Media, 77, 267-285.*

Ibrahim, S. M., Kumar, P. V., Lorenzini, G. & Lorenzini, E. (2019). Influence of joule heating and heat source on radiative MHD flow over a stretching porous sheet with power-law heat flux. *Journal of Engineering Thermophysics*, 28(3), 332–344.

Jaber, K. K. (2016). Joule heating and viscous dissipation on effects on MHD flow over a stretching porous sheet subjected to power law heat flux in presence of heat source. *Open Journal of Fluid Dynamics*, 6(3), 156–165.

Jamshed, W., Devi S, S. U., Goodarzi, M., Prakash, M., Nisar, K.S., Zakarya, M. & Abdel-Aty, A.H. (2021). Evaluating the unsteady casson nanofluid over a stretching sheet with solar thermal radiation: an optimal case study. *Case Studies in Thermal Engineering*, 26, 101160.

Khan, W. A., Khan, M., Irfan, M. & Alshomrani, A. S. (2017). Impact of melting heat transfer and nonlinear radiative heat flux mechanisms for the generalized burgers fluids. *Results Physics*,7, 4025–4032.

Krishna, Y. H., Reddy, G. V. R. & Makinde, O. D. (2018). Chemical reaction effect on mhd flow of casson fluid with porous stretching sheet. *Defect and Diffusion Forum*, 389, 100–109.

Lund, L.A., Omar, Z., Khan, I., Baleanu, D. & Nisar, K.S. (2020). Dual similarity solutions of MHD stagnation point flow of casson fluid with effect of thermal radiation and viscous dissipation: stability analysis. *Scientific Reports*, 10, 15405.

Maraj, E. N., Faizan, U. & Shaiq, S. (2019). Influence of joule heating and partial slip on casson nanofluid transport past a nonlinear stretching planar sheet. *International Conference on Applied and Engineering Mathematics, ICAEM 2019 - Proc.*, 31–36.

Merkin , J. H. (1980). Mixed convection boundary layer flow on a vertical surface in a saturated porous medium. *Journal of Engineering Mathematics*,14(4), 301–313.

Mishra, G. S., Hussain, M.R., Seth, S.M. & Makinde, O.D. (2020). Stability analysis and dual multiple solutions of a hydromagnetic dissipative flow over a stretching / shrinking sheet. *Bulgarian Chemical Communications*, 52(2), 259–271.

Najib, N., Bachok, N. & Arifin, N. M. (2017). Stability of dual solutions in boundary layer flow and heat transfer over an exponentially shrinking cylinder. *Indian Journal of Science and Technolology*, 9(48).

Nandeppanavar, M.M., M.C., K. & Raveendra, N. (2021). Double-diffusive free convective flow of casson fluid due to a moving vertical plate with non-linear thermal radiation. *World Journal of Engineering*, 18(1), 85-93.

Oke, A.S., Mutuku, W.N., Kimathi, M. & Animasaun, I.L. (2020). Insight into the dynamics of non-newtonian casson fluid over a rotating non-uniform surface subject to coriolis force. *Nonlinear Engineering*, 9(1), 398-411.

Salleh, M.Z., Nazar, R. & Pop, I. (2010). Mixed convection boundary layer flow from a solid shpere with newtonian heating in a micropolar fluid. *SRX Physics*, vol. 2010, 736039.

Saidulu, N. & Lakshmi, A. V. (2017). MHD flow of casson fluid with slip effects over an exponentially porous stretching sheet in presence of thermal radiation, viscous dissipation and heat source/sink. *Asian Research Journal of Mathematics*, 2, 1–15.

Salleh, S. N. A., Bachok , N., Arifin, N. M., Ali, F. M. & Pop, I. (2018). Stability analysis of mixed convection flow towards a moving thin needle in nanofluid. *Applied Sciences*, 8(6).

Sarkar, T., Reza-E-Rabbi, S., Artifuzzaman, S.M., Ahmed, R., Khan, M.S. & Ahmmed, S.F. (2019). MHD radiative flow of Casson and Williamson nanofluids over an inclined cylindrical surface with chemical reaction effects. *Int. J. Heat Technol.*, 37, 1117-1126.

Shah, Z., Kumam , P. & Deebani, W. (2020). Radiative MHD casson nanofluid flow with activation energy and chemical reaction over past nonlinearly stretching surface through entropy generation. *Scientific Reports*,10(1),1–14.

Shampine, L., Kierzenka , J. & Reichelt, M. (2000). Solving boundary value problems for ordinary differential equations in MATLAB with bvp4c. *Tutor. Notes*, 75275, 1–27.

Tamoor, M., Waqas, M., Khan, M. I., Alsaedi, A. & Hayat, T. (2017). Magnetohydrodynamic flow of casson fluid over a stretching cylinder. *Results Physics*,7, 498–502.

Vaidya, H., Rajashekhar, C., Manjunatha, G., Prasad, K. V., Makinde, O. D. & Vajravelu K. (2020). Heat and mass transfer analysis of MHD peristaltic flow through a complaint porous channel with variable thermal conductivity. *Physica Scripta*, 95(4).

W, P. D. & Awaludin, A. I. I.S. (2016). Stability analysis of stagnation-point flow over a stretching/shrinking sheet. in *AIP ADVANCES*, 045308.

Zaib, A., Bhattacharyya ,K., Uddin , M. S. & Shafie , S. (2016). Dual solutions of non-newtonian casson fluid flow and heat transfer over an exponentially permeable shrinking sheet with viscous dissipation. *Modelling and Simulation in Engineering*, 2016.

Zehra, I., Abbas, N., Amjad, M., Issakhov, A., Nadeem, S. & Saleem, S. (2021). Casson Nanoliquid flow with Cattaneo-Christov flux analysis over a curved stretching/shrinking channel. *Case Stud. Therm. Eng.* 27, 101146.

Figure

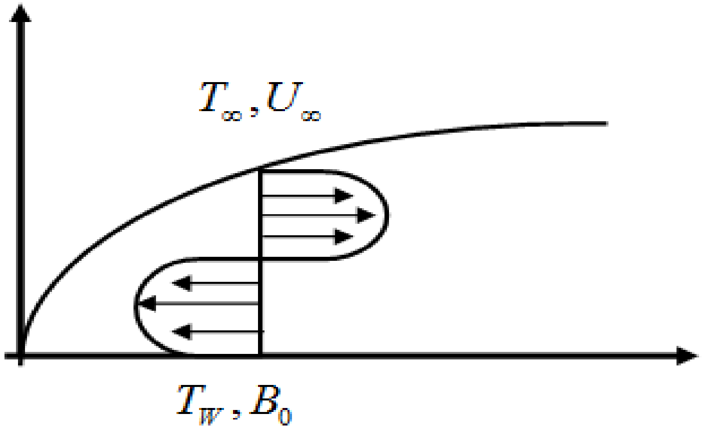

Figure 1 Flow diagram

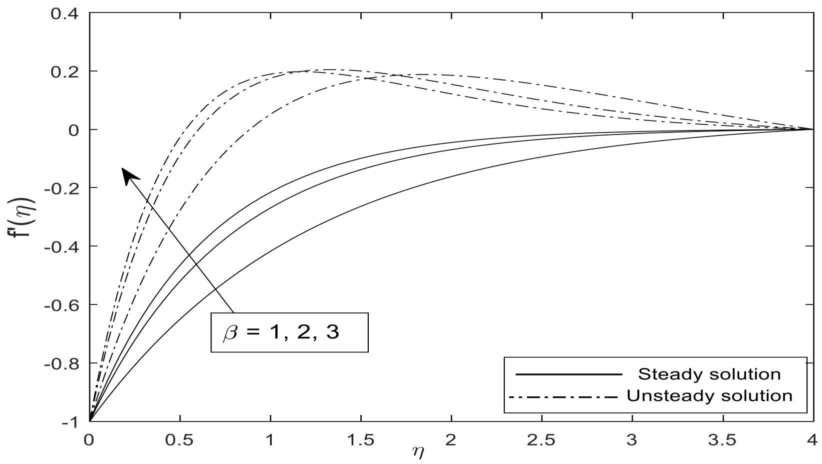

Figure 2 Impact of β on velocity distribution when

$\Pr = 0.72, Ec = 3, J = 1, H = 1, M = 0.2$ & $s = 2.23.$

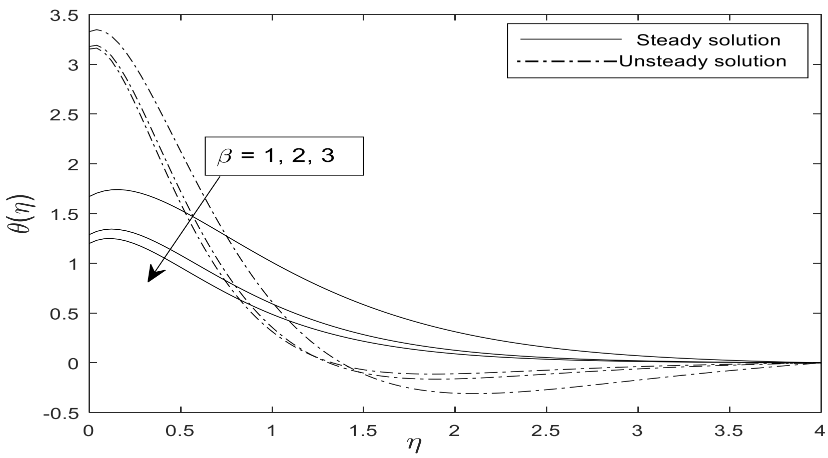

Figure 3 Impact of β on Temperature field when

$\Pr = 0.72, Ec = 3, J = 1, H = 1, M = 0.2$ & $s = 2.23.$

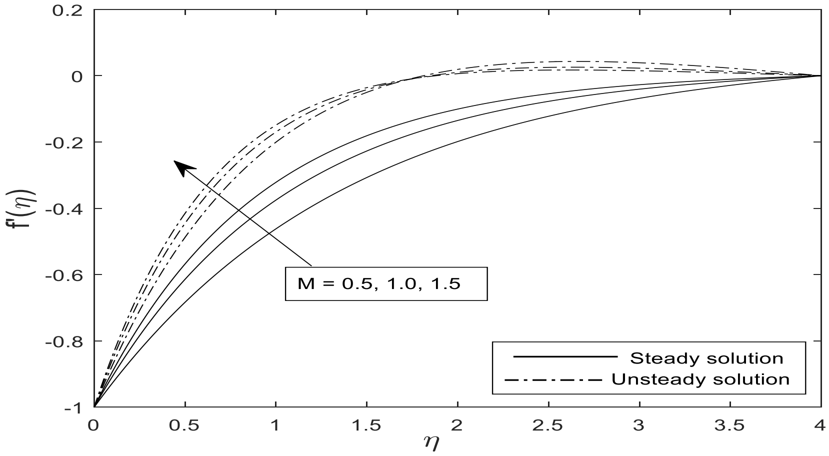

Figure 4 Impact of M on velocity field when

$\Pr = 0.72, Ec = 3, J = 1, H = 1, s = 2.23 \,\&\, \beta = 0.2.$

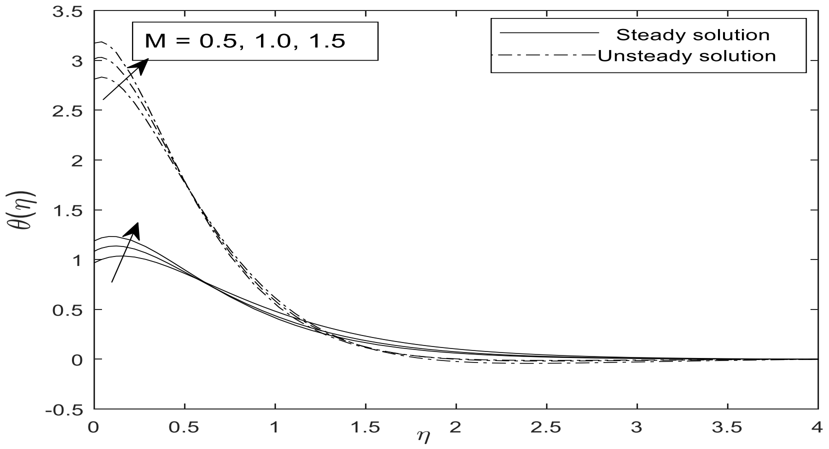

Figure 5 Impact of M on Temperature field when

$\Pr = 0.72, Ec = 3, J = 1, H = 1, s = 2.23 \,\&\, \beta = 0.2.$

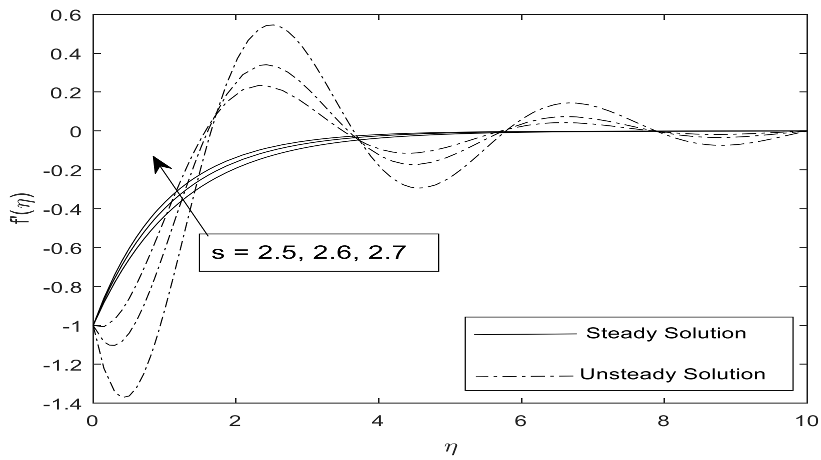

Figure 6 Impact of s on velocity field when

$\Pr = 0.72, Ec = 3, J = 1, H = 1, M = 0.2 \,\&\, \beta = 0.2.$

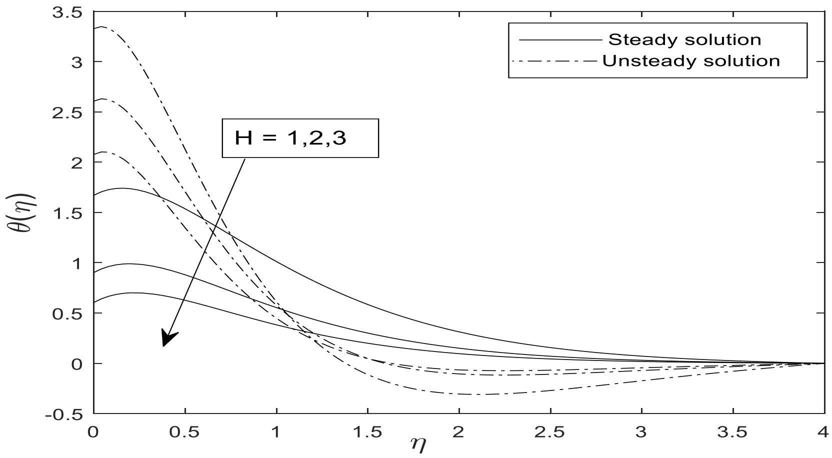

Figure 7 Impact of H on Temperature field when

$\Pr = 0.72, Ec = 3, J = 1, s = 2.23, M = 0.2 \,\&\, \beta = 0.2.$

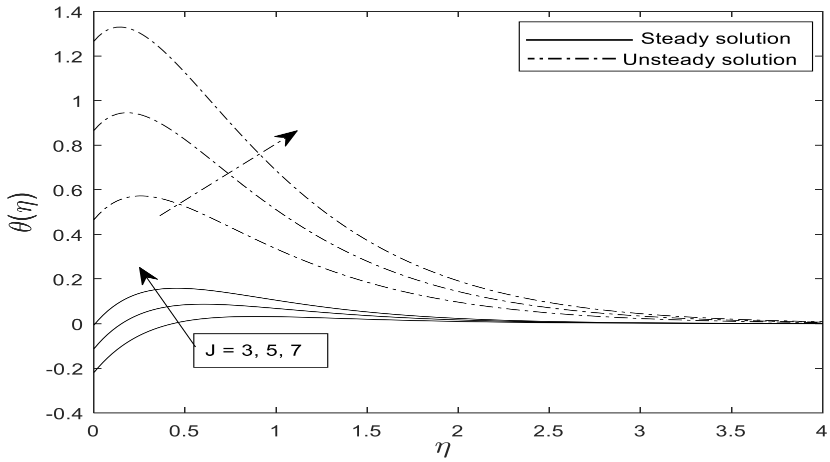

Figure 8 Impact of J on Temperature field when

$\Pr = 0.72, Ec = 3, H = 1, s = 2.23, M = 0.2 \,\&\, \beta = 0.2.$

Table

M	Jaber (2016) works (shooting technique solutions)	Present Results (bvp4c solution)	
		Steady Solution	Unsteady Solution
1.0	2.00007	2.0009	3.0311
3.0	2.56155	2.5616	3.1138
5.0	3.0	3.0	3.5311

Table-1: Numerical values of negative magnitude of skin-friction coefficient $(-C_f)$ **for various values of Magnetic parameter (M) when** $\Pr = 0.72, Ec = 3, J = 1, H = 1 \& s = 1$ **in the case of Newtonian fluid and stretching sheet.**

s	Smallest Eigen-value	
	Steady Solution	Unsteady Solution
2.5	2.5000	-2.3380
2.6	2.6000	-2.1521
2.7	2.7000	-2.7426

Table-2: Numerical values of smallest eigen-values for a range of suction parameter (s) when $\Pr = 0.72, Ec = 3, J = 1, H = 1, M = 0.2 \& \beta = 0.2.$